



BI 1291583: a novel selective inhibitor of cathepsin C with superior in vivo profile for the treatment of bronchiectasis

Stefan Kreideweiss¹ · Gerhard Schänzle¹ · Gisela Schnapp¹ · Viktor Vintonyak¹ · Marc A. Grundl¹

Received: 7 February 2023 / Revised: 26 June 2023 / Accepted: 24 July 2023 / Published online: 4 August 2023
© The Author(s) 2023

Abstract

Background Airway inflammation in chronic inflammatory lung diseases (e.g. bronchiectasis) is partly mediated by neutrophil-derived serine protease (NSP)/antiprotease imbalance. NSPs are activated during neutrophil myelopoiesis in bone marrow by cathepsin C (CatC; DPP1). CatC is therefore an attractive target to reduce NSP activity in the lungs of patients with bronchiectasis, restoring the protease/antiprotease balance. We report results from the preclinical pharmacological assessment of the novel CatC inhibitor BI 1291583.

Methods Binding kinetics of BI 1291583 to human CatC were determined by surface plasmon resonance. In vitro inhibition of human CatC activity was determined by CatC-specific fluorescent assay, and selectivity was assessed against related cathepsins and unrelated proteases. Inhibition of NSP neutrophil elastase (NE) production was assessed in a human neutrophil progenitor cell line. In vivo inhibition of NE and NSP proteinase 3 (PR3) in bronchoalveolar lavage fluid (BALF) neutrophils after lipopolysaccharide (LPS) challenge and distribution of BI 1291583 was determined in a mouse model.

Results BI 1291583 bound human CatC in a covalent, reversible manner, selectively and fully inhibiting CatC enzymatic activity. This inhibition translated to concentration-dependent inhibition of NE activation in U937 cells and dose-dependent, almost-complete inhibition of NE and PR3 activity in BALF neutrophils in an in vivo LPS-challenge model in mice. BI 1291583 exhibited up to 100 times the exposure in the target tissue bone marrow compared with plasma.

Conclusion BI 1291583-mediated inhibition of CatC is expected to restore the protease–antiprotease balance in the lungs of patients with chronic airway inflammatory diseases such as bronchiectasis.

Keywords Preclinical · Cathepsin C inhibitor · Bronchiectasis · Neutrophil-derived serine protease activity

Abbreviations

BALF	Bronchoalveolar lavage fluid	k_{off}	Mean dissociation rate constant
CatC	Cathepsin C	LPS	Lipopolysaccharide
CatG	Cathepsin G	NE	Neutrophil elastase
ED ₅₀	Effective dose of drug that inhibits 50% of target activity	NSP	Neutrophil-derived serine protease
ED ₉₉	Effective dose of drug that inhibits 99% of target activity	PR3	Proteinase 3
IC ₅₀	Concentration of drug resulting in 50% inhibition of target	RFU	Relative fluorescence units
K _D	Equilibrium dissociation constant	SEM	Standard error of mean
k_{on}	Mean association rate constant	$t_{1/2}$	Half-life ($t_{1/2}$)

Responsible Editor: Bernhard Gibbs.

✉ Marc A. Grundl
marc.grundl@boehringer-ingenheim.com

¹ Boehringer Ingelheim Pharma GmbH & Co. KG, Biberach, Germany

Background

Bronchiectasis is a disease of the lower respiratory tract that is caused by a wide range of underlying clinical disorders [1]. Underlying aetiologies range from well-characterised genetic diseases such as cystic fibrosis (CF) and primary ciliary dyskinesia, to asthma, chronic obstructive pulmonary disease and post-infectious sequelae as well as various autoimmune diseases. However, the single largest aetiology

is idiopathic bronchiectasis, in which the underlying cause is unknown [1]. While each underlying aetiology considered individually may be rare, taken together, bronchiectasis occurs in up to 94.8 people per 100,000 (0.1%) [2], increasing with age and female gender [3]. Prevalence is growing, and bronchiectasis has been described as an emerging global epidemic [4, 5].

Bronchiectasis is characterised by abnormal, scarred and irreversibly dilated bronchi [6]. The pathogenesis is not fully understood; however, once established, patients show evidence of chronic inflammation, infection, impaired mucociliary clearance and progressive structural lung damage. The complex interaction between these features (the so-called “vicious vortex”) leads to exacerbations and decline in pulmonary function, with associated morbidity and mortality [1].

Neutrophilic inflammation is a central feature of bronchiectasis, the extent of which has been associated with disease severity and progression [7, 8]. The release of inflammatory effectors from neutrophils contributes toward the inflammatory environment of the lung [9], and an imbalance between neutrophil-derived serine proteases (NSPs; neutrophil elastase [NE], proteinase 3 [PR3] and cathepsin G [CatG]) and their endogenous inhibitors has been documented in patients with chronic inflammatory respiratory diseases, including bronchiectasis [10–14]. This imbalance has been shown to impair defence against bacterial infection, impair mucociliary clearance, promote mucus hypersecretion and degrade elastin and other extracellular matrix components [10, 15]. NE has been shown to inhibit ciliary function and mucociliary clearance as well as promote mucus secretion in vitro, and NE activity in sputum is associated with disease severity, increased susceptibility to airway bacterial colonisation, increased risk/frequency of exacerbations, hospitalisations and mortality [16–19]. Levels of PR3 in sputum were found to be raised in patients with bronchiectasis during exacerbations compared with stable disease (i.e. not during an exacerbation) [20]. Additionally, PR3 concentration was correlated with levels of NE in sputum [20]. CatG has been implicated in the pathogenesis of bronchiectasis, resulting in destruction of airway epithelium and dysfunction of ciliated cells [21]. Increased CatG activity has been observed in patients with bronchiectasis compared with controls, with CatG activity increasing with increasing disease severity [21].

NE, PR3 and CatG are activated by cathepsin C (CatC; also known as dipeptidyl peptidase 1) during myelopoiesis of neutrophils in the bone marrow [22]. In the neutrophil progenitor cells, these NSPs are synthesised as pre-proenzymes that are trafficked to lysosomes, where they then are cleaved into proenzymes, finally activated by the removal of a prodipeptide by CatC into active mature enzymes and stored under acidic conditions (pH 4–5); non-activated NSPs

are degraded prior to release of the mature neutrophils from the bone marrow [10, 22]. Inhibition of CatC in the bone marrow is therefore expected to result in circulating neutrophils with decreased levels of active NSPs recruited to the lungs of patients with chronic inflammatory lung diseases such as bronchiectasis. This, in turn, is expected to reduce distal airway destruction by enzymatic degradation of pulmonary elastin and connective tissue; possible secondary anti-inflammatory and anti-mucus hypersecretory effects are also expected [18, 23–25].

Currently available treatments for bronchiectasis, such as antibiotics, mucolytics and anti-inflammatories, are symptomatic only, with no drug licensed for treatment of the underlying pathophysiology, and the only evidence-based intervention to date is chest clearance [26, 27]. Further, in many cases, antibiotic treatment is insufficient to control infection, and even in the absence of infection, inflammation can progress [28]. Therefore, there is a high medical need for a novel treatment that breaks the vicious vortex of neutrophilic inflammation, prevents exacerbations and improves symptoms. Based on the aforementioned biology, inhibition of CatC is expected to have that potential. First evidence comes from the CatC inhibitor brensocatib (formerly AZD7986), which is currently in Phase 3 development for bronchiectasis (NCT04594369) [29]. BI 1291583 is a novel, highly potent and selective CatC inhibitor under investigation as a potential disease-modifying therapy for patients with bronchiectasis. In this study, we report the pre-clinical pharmacological in vitro and in vivo characterisation of BI 1291583.

Methods

A brief summary of methods is given below. For detailed methodology, see Additional File 1. GraphPad Prism software (version 9.5.0 for Windows, GraphPad Software, www.graphpad.com) was used to generate all graphical representations of the data.

Binding kinetics of BI 1291583 to human CatC

Binding kinetics of BI 1291583 to human CatC were assessed by surface plasmon resonance using a Biacore T200 system. Activated human CatC was immobilised on a CM5 chip using standard procedures. Increasing concentrations of BI 1291583 (0.08, 0.4, 2, 10 and 50 nM) were then injected onto the immobilised target at pH 4.5. Mean association rate constant (k_{on}) and dissociation rate constant (k_{off}) values were calculated from three individual experiments using Biacore T200 Evaluation Software, Version 1.0, 2010. The equilibrium dissociation constant (K_D) was calculated from k_{off}/k_{on} , and half-life ($t_{1/2}$) was calculated by \ln_2/k_{off} .

In vitro inhibition of recombinant human cathepsin enzymatic activity

Activity of recombinant human cathepsins in the presence of BI 1291583 was measured by conversion of fluorescent substrates for cathepsins C, K and L (duplicate experiments), and F, B, H and S (single experiments). Activated cathepsins were incubated with serial dilutions of BI 1291583 followed by addition of fluorescent cathepsin substrates. The reaction was stopped by addition of an inhibitor compound and fluorescence levels measured with an Envision Reader at excitation wavelength 355 nm, emission wavelength 460 nm, with vehicle controls as reference for non-inhibited enzyme activity and inhibitor as control for background fluorescence. Changes in fluorescence resulting from BI 1291583-mediated inhibition of cathepsins were determined by calculating the percentage of fluorescence in the presence of BI 1291583 compared with the fluorescence of the vehicle control after subtracting the background fluorescence. The concentration of BI 1291583 that inhibited 50% of cathepsin activity (IC_{50}) was calculated using GraphPad Prism software (version 9.5.0 for Windows, GraphPad Software, www.graphpad.com) with a non-linear regression curve fit.

Inhibition of the production of active NE in a neutrophil progenitor cell line

The inhibitory activity of BI 1291583 on the production of active NE was investigated in duplicate experiments in the human myeloid cell line U937. U937 cells were used as they constitutively express and process NE. Additionally, a myeloid cell line was used rather than primary neutrophils as CatC activates NSPs in the bone marrow during myelopoiesis and no further activation occurs once the neutrophils have entered the bloodstream; as such, the effect of CatC inhibition cannot be investigated in primary neutrophils. BI 1291583 was added to cell suspensions at a final concentration of 0.064, 0.32, 1.6, 8, 40, 200 and 1000 nM. Cells were then incubated for 48 h. Cell viability was then measured in duplicate experiments using the CellTiter-Glo[®] Luminescent Cell Viability Assay according to manufacturer's instructions. For measurement of NE activity, cells were separated by centrifugation, lysed and debris removed. NE activity was measured by conversion of a fluorescent substrate. Increase in fluorescence was measured over time with a SpectramaxM5 fluorescence reader at 360 nm excitation wavelength and 460 nm emission wavelength. The reaction rate when CatC is fully saturated by BI 1291583 was used as primary readout to calculate NE activity. Percentage inhibition of NE activity in lysates treated with BI 1291583 was calculated relative to the mean of the vehicle-only control. IC_{50} was calculated using GraphPad Prism software

(version 9.5.0 for Windows, GraphPad Software, www.graphpad.com) with a non-linear regression curve fit.

The inhibitory effect of INS1007 (the active component of brensocatib) on the production of active NE was investigated under the same conditions (see Methods, Additional File 1).

In vivo inhibition of the production of active NE, CatG and PR3

To demonstrate the ability of BI 1291583 to block the production of active NSPs, an in vivo proof-of-mechanism model was established in mice (female Crl:NMRI mice [$n=6$ per treatment group]), and two dosing schedules were carried out. In the first—a 2-day treatment holiday regimen—mice were treated with 0.005, 0.05, 0.5 or 5 mg/kg BI 1291583, or vehicle, twice daily by oral gavage on Days 1–5, 8 and 9. On Day 10, a final dose of BI 1291583 or vehicle was given followed by challenge with nebulised *E. coli* lipopolysaccharide (LPS) to induce neutrophil influx into the lungs. In the second dosing regimen, mice were treated with 0.00005, 0.0001, 0.001, 0.01, 0.03, 0.1, 0.5 or 5 mg/kg BI 1291583, or vehicle, once daily by oral gavage for 11 consecutive days. On Day 12, a final dose of BI 1291583 or vehicle was given followed by LPS challenge.

Four and a half hours after LPS challenge, lung neutrophils were harvested by lavage via tracheal cannula, and neutrophil count measured. Bronchoalveolar lavage fluid (BALF) samples were then centrifuged and cell pellets lysed with volume of lysis buffer normalised to neutrophil count. NE, CatG and PR3 activity were determined by conversion of a fluorescent substrate measured over time with a SpectramaxM5 fluorescence reader at 360 nm excitation wavelength and 460 nm emission wavelength. Fluorescence values were normalised to neutrophil count, and mean NE, CatG and PR3 activity from BI 1291583-treated animals was calculated relative to the mean of LPS/vehicle-treated control animals. CatG and PR3 activity was measured in pooled samples from each dose group. For the 11-day dosing experiments, the dose of BI 1291583 that inhibited 50% of NE activity (ED_{50}) was calculated using GraphPad Prism software (version 9.5.0 for Windows, GraphPad Software, www.graphpad.com) with a non-linear regression curve fit. The dose inhibiting 99% of NE activity (ED_{99}) was calculated from the regression curve using the equation $ED_{99} = 99^{(1/\text{hill slope})} \times ED_{50}$. A one-way analysis of variance with Dunnett's multiple comparisons test analysis was performed to determine statistical significance.

At 5 h after final BI 1291583 administration, animals were euthanised by Narcoren application (400–600 mg/kg intraperitoneally). For assessment of BI 1291583 exposure in plasma, five drops of retrobulbar blood were taken. The femur was prepared by extraction, shock frozen in liquid

nitrogen and stored at $-20\text{ }^{\circ}\text{C}$ until bone marrow preparation. For preparation of bone marrow, epiphysis severed off and bone marrow extracted from the diaphysis. Exposure was measured via liquid chromatography–tandem mass spectrometry.

The inhibitory activity of INS1007 on the production of active NE, and distribution of INS1007 to bone marrow and plasma was investigated under the same conditions as the 11-day dosing regimen (see Methods, Additional File 1).

Selectivity analysis against unrelated proteases

Inhibitory and stimulatory activity of BI 1291583 (10 μM) against a panel of unrelated proteases from different classes was assessed by enzyme assays, using validated fluorometric or photometric techniques as appropriate. Effect was calculated as percentage inhibition (positive values) or stimulation (negative values) of a control inhibitor for each protease. An inhibition or stimulation of less than 25% was considered as insignificant, 25–50% was considered weak to moderate, and greater than 50% was considered significant. Experiments were carried out in duplicate and results presented as mean values.

Results

BI 1291583 binds human CatC in a reversible manner

BI 1291583 bound recombinant human CatC with mean k_{on} and k_{off} values at pH 4.5 of $6.36 \times 10^6\text{ M}^{-1}\text{ s}^{-1}$ and $2.29 \times 10^{-3}\text{ s}^{-1}$, respectively, yielding a KD value of 0.43 nM. Mean $t_{1/2}$ was 5.19 min. Kinetic parameters are summarised in Additional File 1: Table AF1.

BI 1291583 selectively inhibits human CatC enzymatic activity in vitro

Human CatC was inhibited with a mean IC_{50} of 0.9 nM (Fig. 1), with high selectivity among other related cysteine proteases (IC_{50} values ranging from 6695 nM for cathepsin K to greater than 100,000 nM for cathepsins B, F and H) (Table 1). Rat and mouse CatC were inhibited with similar potencies (mean IC_{50} values of 1.2 nM and 0.6 nM, respectively).

BI 1291583 does not inhibit or stimulate other unrelated proteases

No relevant inhibition or stimulation of 33 unrelated proteases from four different classes was detected at 10 μM (Additional File 1: Table AF2).

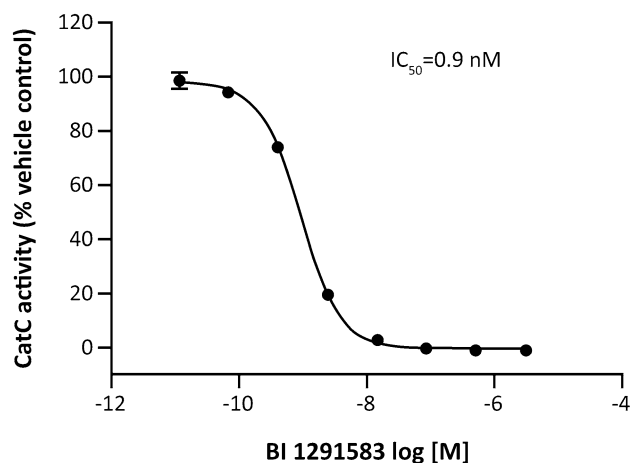


Fig. 1 Inhibition of recombinant human CatC by BI 1291583. CatC cathepsin C, IC_{50} concentration of BI 1291583 resulting in 50% inhibition of cathepsin C enzymatic activity. Data are mean. Error bars depict standard deviation across duplicate experiments

Table 1 Comparison of BI 1291583 enzyme selectivity for recombinant human cathepsins

Enzyme	IC_{50} , nM
Cathepsin C	0.9
Cathepsin B	> 100,000
Cathepsin F	> 100,000
Cathepsin H	> 100,000
Cathepsin K	6695
Cathepsin L	7225
Cathepsin S	25,200

IC_{50} concentration of BI 1291583 resulting in 50% inhibition of cathepsin enzymatic activity

BI 1291583 inhibits the production of active NE in a neutrophil progenitor cell line

BI 1291583 inhibited the production of active NE in neutrophil progenitor U937 cells in a concentration-dependent manner, with a mean IC_{50} of 0.7 nM, with no effects on cell viability (cell viability > 93% at all concentrations of BI 1291583 and a mean cell viability of 98% at the highest concentration [1000 nM]) (Fig. 2).

BI 1291583 inhibits the production of active NE, PR3 and CatG in vivo

In vivo efficacy was evaluated in an LPS-challenge model in mice. In the 2-day treatment holiday regimen, BI 1291583 inhibited production of active NE in mouse BALF neutrophils in a dose-dependent manner up to a maximum of 97%. For NE analysis, BALF neutrophil lysates from animals treated with vehicle only and twice-daily dosing of 0.005,

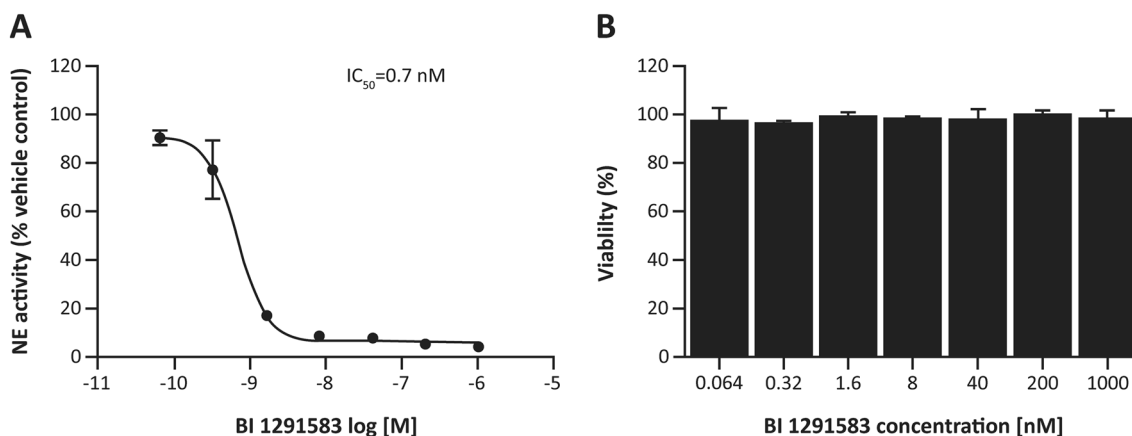


Fig. 2 **A** Inhibition of the production of active NE in U937 cells by BI 1291583 and **B** effect on cell viability. IC_{50} concentration of BI 1291583 resulting in 50% inhibition of activation of neutrophil

elastase, *NE* neutrophil elastase. Data are mean. Error bars depict standard deviation across duplicate experiments

0.05, 0.5 and 5 mg/kg BI 1291583 yielded mean (standard error of mean [SEM]) fluorescence signals of 2118.1 (132.3), 1008.3 (176.5), 458.1 (165.0), 81.1 (57.3) and 62.9 (46.8) relative fluorescence units (RFU) per 10^5 neutrophils, respectively. These values translate to significant ($p < 0.001$) 44% (8.3%), 75% (7.8%), 96% (2.7%) and 97% (2.2%) inhibitions compared with vehicle-only treatment (Additional File Figure AF1, part A). An ED_{99} value for NE inhibition was calculated at 1.5 mg/kg. For CatG analysis, V_{max} values for vehicle only and 0.005, 0.05, 0.5 and 5 mg/kg BI 1291583 were 0.79, 0.28, 0.05, 0.01 and 0.01/ 10^5 neutrophils, respectively, translating to 65%, 94%, 99% and 99% inhibitions compared with vehicle-only treatment (Additional File Figure AF1, part B).

Treatment with BI 1291583 for 11 days had no effect on LPS-induced neutrophil influx into the lung, but almost completely (99%) inhibited production of active NE in a dose-dependent manner. For NE analysis, BALF neutrophil lysates from animals treated with vehicle only and daily dosing of 0.1 mg/kg, 0.5 mg/kg and 5 mg/kg BI 1291583 yielded mean (SEM) fluorescence signals of 1419.2 (198.3),

147.8 (87.5), 27.0 (16.9) and 15.5 (4.6) relative fluorescence units (RFU) per 10^5 neutrophils, respectively. These values translate to significant ($p < 0.001$) 90% (6.2%), 98% (1.2%) and 99% (0.3%) inhibitions compared with vehicle-only treatment (Fig. 3). The ED_{50} value for NE inhibition was calculated at 0.03 mg/kg, and ED_{99} was calculated at 0.3 mg/kg (Fig. 4). For PR3 analysis, values (SEM) for vehicle only and 0.1, 0.5 and 5 mg/kg BI 1291583 were 182 (47.5), 19 (0), 13.5 (1.5) and 10 (1.0) RFU/ 10^5 neutrophils, respectively, translating to significant mean 90% (0%), 93% (0.8%) and 94% (0.6%) inhibitions compared with vehicle-only treatment (all $p < 0.001$) (Fig. 5).

BI 1291583 distributes preferentially to bone marrow

At approximately 5 h after the final dose of BI 1291583 on Day 10 of 2-day treatment holiday regimen, mean (SEM) BI 1291583 exposure in bone marrow at 0.5 mg/kg was 2981.7 (185.0) nM. In plasma, the corresponding value was 32.5

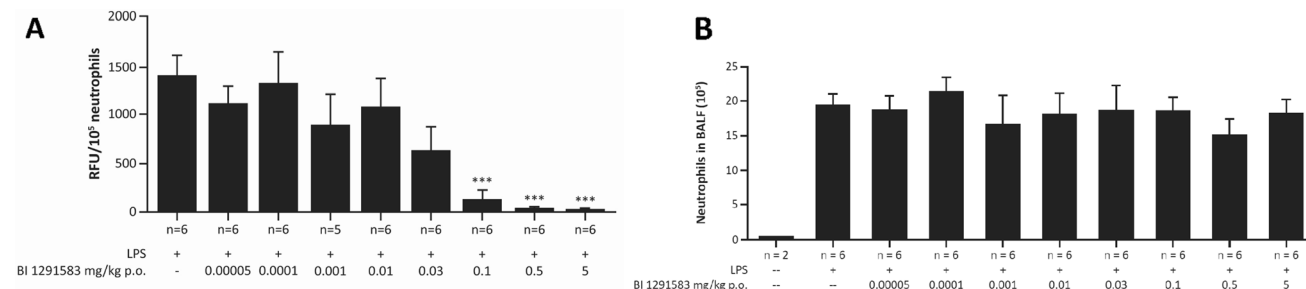


Fig. 3 Effect of treatment with BI 1291583 on **A** NE activity in mouse BALF neutrophil lysate and **B** absolute neutrophil numbers in BALF after LPS challenge, 11-day dosing. *BALF* bronchoalveo-

lar lavage fluid, *LPS* lipopolysaccharide, *NE* neutrophil elastase, *p.o.* orally, *RFU* relative fluorescence units. *** $p < 0.001$ compared with vehicle. Data are mean. Error bars indicate standard error of the mean

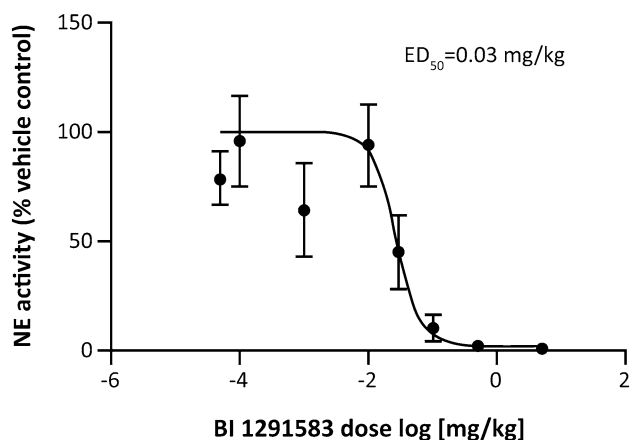


Fig. 4 Dose–response for inhibition of active NE production in mouse BALF neutrophil lysate after treatment with BI 1291583 and subsequent LPS challenge, 11-day dosing. ED_{50} effective dose that inhibits 50% of production of active neutrophil elastase, NE neutrophil elastase. Data are mean. Error bars depict standard error of the mean

(2.1) nM. This equates to a bone marrow-to-plasma exposure ratio of approximately 92 (Additional File Figure AF2).

At 5 h after the final dose of BI 1291583 on Day 12 of the 11-day dosing regimen, mean (SEM) BI 1291583 exposure in bone marrow at efficacious doses (0.1, 0.5, 5 mg/kg) was 428.5 (83.6) nM, 1973.2 (908.9) nM and 11,092.0 (3287.5) nM, respectively. In plasma, corresponding values were 3.5 (0.4) nM, 24.2 (1.6) nM and 342.8 (24) nM. This equates to bone marrow-to-plasma exposure ratios of 122, 82 and 32 (Fig. 6).

The results of experiments investigating effects of INS1007 on production of active NE in U937 cells and the mouse LPS-challenge model, and analysis of distribution to bone marrow and plasma, can be found in Additional File 1.

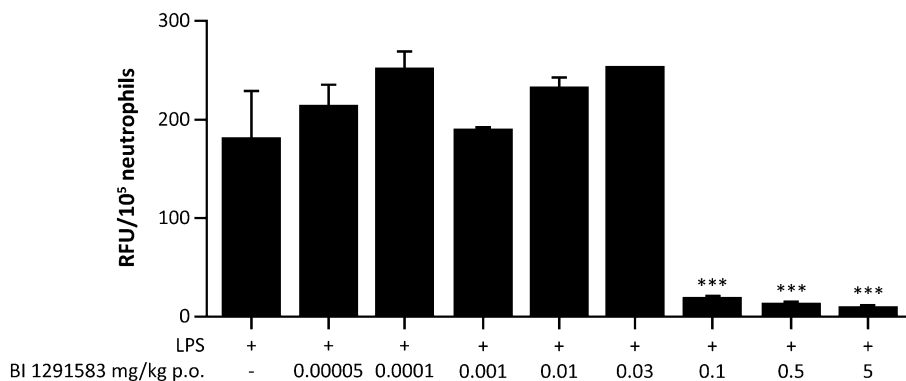


Fig. 5 PR3 activity in mouse BALF neutrophil lysate after treatment with BI 1291583 and subsequent LPS challenge, 11-day dosing. BALF bronchoalveolar lavage fluid, LPS lipopolysaccharide, *p.o.* orally, RFU relative fluorescence units, PR3 proteinase 3.

Discussion

In this comprehensive preclinical analysis, we demonstrated that BI 1291583 is a potent and selective inhibitor of CatC. Using SPR data, we could show that BI 1291583 binds human CatC in a reversible manner. It fully inhibited human recombinant CatC with a selectivity of greater than 6000-fold compared with a panel of related cathepsins, in addition to no relevant inhibition or stimulation of unrelated proteases from different classes. We also demonstrated similar potencies with mouse and rat CatC. We were then able to show that BI 1291583 had relevant downstream effects, dose-dependently inhibiting the production of active NE in a neutrophil progenitor cell line with no effect on cell viability. Finally, in the 2-day treatment holiday regimen, we demonstrated that BI 1291583 dose-dependently inhibited the production of active NE and CatG in BALF neutrophils by up to 97% and 99%, respectively. In the 11-day consecutive dosing model, we also demonstrated that BI 1291583 inhibited production of active NE and PR3 by up to 99% and 94%, respectively. At efficacious doses (those resulting in statistically significant inhibition of NSPs), BI 1291583 distributed to the target compartment of the bone marrow at up to 100 times the exposure compared with plasma, a property that can potentially be beneficial in reducing the risk of side effects due to the inhibition of CatC outside the bone marrow in patients.

There are few CatC inhibitors that have reached the level of clinical trials, and only two other compounds still in clinical development in bronchiectasis. HSK31858 is a CatC inhibitor that is currently being assessed in a Phase 2 clinical trial in patients with non-CF bronchiectasis (NCT05601778). Brensocatib (formerly AZD7986) is an

*** $p < 0.001$ compared with vehicle. Samples were pooled for analysis of PR3 activity. Data are mean. Error bars depict standard error of the mean across duplicate experiments

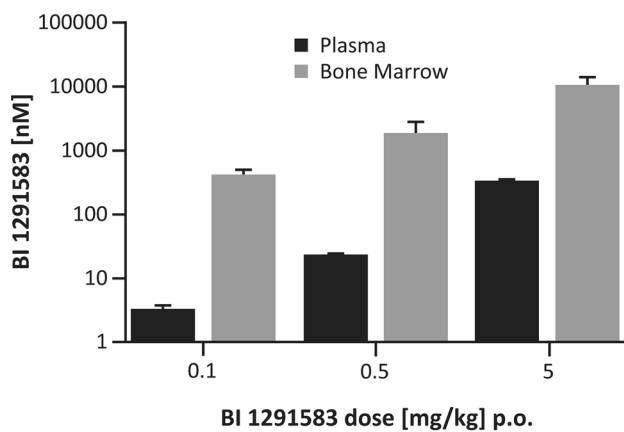


Fig. 6 Bone marrow and plasma distribution of BI 1291583 at 5 h post-administration, 11-day dosing, *p.o.* orally. Data are mean. Error bars depict standard error of the mean

oral, reversible CatC inhibitor currently in Phase 3 development for patients with bronchiectasis (NCT04594369). In Phase 1 development, healthy volunteers were randomised to once-daily doses of either brensocatic up to 40 mg or placebo for up to 28 days, and followed up for 1 month [30]. Exposure-related reduction in NE activity was demonstrated, with a generally well-tolerated safety profile; however, several dose-dependent, possibly CatC-related non-serious skin findings (exfoliation and hyperkeratosis) were observed [30]. In a subsequent Phase 2 trial [31], patients with bronchiectasis who had had at least two exacerbations in the previous year were randomised to once-daily doses of either 10 mg or 25 mg brensocatic or placebo for 24 weeks. Compared with placebo, at both brensocatic dose levels, the time to first exacerbation was significantly increased, risk of exacerbation was lower over the treatment period, and both annualised rates of exacerbations and the number of severe exacerbations were lower [31]. As in Phase 1 development, the incidence of hyperkeratosis was higher in the brensocatic-treated groups compared with the placebo group [31].

Brensocatic is at an advanced stage of clinical development. However, data presented here in the light of published data for brensocatic [32] suggest that BI 1291583 may also be a promising candidate for the treatment of patients with chronic inflammatory lung diseases, including bronchiectasis. We demonstrate that BI 1291583 inhibited recombinant human CatC with an IC_{50} of 0.9 nM; the published value for brensocatic is 4.0 nM [32]. Further, we have carried out an in-house analysis of INS1007—the active ingredient of brensocatic—under the same conditions as for BI 1291583, examining inhibition of NE in U937 cells, and NE inhibition and distribution to plasma and bone marrow in an in vivo mouse model (see Additional File 1). In this analysis, INS1007 inhibited the production of active NE in U937 cells

with an IC_{50} of 64 nM; the value for BI 1291583 demonstrated in the study presented here is 0.7 nM. In the LPS challenge mouse model, INS1007 was tested at doses for which BI 1291583 resulted in statistically significant inhibition of NSPs for BI1291583 (0.1, 0.5 and 5 mg/kg). Overall, for INS1007, lower levels of inhibition of NE activation were observed compared with levels reported for BI 1291583 in this study (Additional File 1, Fig AF3). At the highest dose (5 mg/kg), INS1007 achieved up to 76% inhibition of NE activation in BALF neutrophils compared with vehicle control. BI1291583 shows 99% inhibition of NE activity at this dose (Additional File Figure AF4). At a low dose of 0.1 mg/kg, BI 1291583 resulted in 90% inhibition, whereas the same dose of INS1007 resulted in no inhibition, in line with the observed in vitro potencies. Analysis of INS1007 exposure at approximately 5 h after dosing at 0.1 mg/kg, 0.5 mg/kg and 5 mg/kg likewise revealed markedly lower bone marrow-to-plasma exposure ratios than those we report here for BI 1291583 (28, 4 and 2, respectively, for INS1007; 122, 81 and 32, respectively, for BI 1291583) (Additional File Figure AF5).

Overall, data from this in-house analysis of INS1007 strengthen the suggestion that BI 1291583 will be a promising candidate for the treatment of bronchiectasis, with a high bone marrow-to-plasma distribution ratio, high efficacy in both U937 cells and in vivo, and very low efficacious plasma concentrations, suggesting high target compartment efficacy.

In the present study, we demonstrate the bone marrow-to-plasma distribution profile of BI 1291583 in a mouse model. To investigate any interspecies differences in exposure, we carried out separate comparative kinetic studies in mice and rats after a single oral dose. In both species, we observed rapid distribution of BI 1291583 into bone marrow, with slow depletion (Additional File Figure AF6). Likewise, high bone marrow-to-plasma exposure ratios were observed, even at low doses, with no obvious difference between species. These data suggest that BI 1291583 has a rapid distribution into the target tissue in vivo, and complement the in vivo observations in both the 2-day treatment holiday regimen, and after 11 consecutive days of dosing in the present study.

A role for CatC in maintaining the structural integrity of plantar and palmar epidermal surfaces has been suggested, through processing of keratins in keratinocytes [33]. This suggestion is supported by the observation of dose-dependent skin events in the Phase 1 study of brensocatic [30]—the relative rapidity of onset of these events did not correlate with the dynamics of NE activity. Further, in the Phase 1 study of the irreversible CatC inhibitor GSK2793660 [34], marked skin desquamation events were observed along with insufficient inhibition of downstream NSPs, which led to trial termination. We suggest that the preferential distribution of BI 1291583 to the bone marrow observed in our study may minimise skin events in subsequent clinical trials.

Increased levels of sputum PR3 have been previously demonstrated alongside NE in patients with bronchiectasis during exacerbations [20]; similarly, CatG has also been implicated in the pathogenesis of bronchiectasis alongside NE [21]. Thus, our finding of a dose-dependent significant decrease in production of active PR3 and CatG *in vivo* by BI 1291583 suggests that upstream inhibition of CatC, and the resulting broad inhibition of NSPs, may add further beneficial therapeutic potential in patients with bronchiectasis.

Conclusion

This study demonstrates that BI 1291583 is a reversible, highly potent and highly selective inhibitor of CatC, which has the potential to ameliorate neutrophilic inflammation and tissue destruction mediated by uncontrolled NSP activity in the airways. Results of this preclinical study support further clinical investigation of BI 1291583 in patients with bronchiectasis.

Supplementary Information The online version contains supplementary material available at <https://doi.org/10.1007/s00011-023-01774-4>.

Acknowledgements The authors would like to thank Yvette Hoevels, Susanne Edele, Ingrid Christ, Diana Edelhäuser, Helga Dolpp, Ramona Schönbrodt, Philipp Rechtsteiner, Dragica Blasevic and Dunja Budweiser for their excellent technical assistance during the conduct of these studies. Lee Kempster, PhD of Meditech Media provided writing, editorial support, and formatting assistance, which was contracted and funded by BI. BI was given the opportunity to review the manuscript for medical and scientific accuracy as well as intellectual property considerations.

Author contributions SK designed, supervised and evaluated the *in vitro* experiments (enzyme activity assay, selectivity assays, U937 assay) and *in vivo* studies; GS designed, supervised and evaluated binding kinetic experiments; VV designed and supervised the synthesis of inhibitor compound BI 1291583; MG analysed and interpreted *in vitro* and *in vivo* data; designed and supervised discovery and synthesis of inhibitor compound BI 1291583. The authors meet criteria for authorship as recommended by the International Committee of Medical Journal Editors (ICMJE). The authors did not receive payment related to the development of the manuscript.

Funding The analyses were supported and funded by Boehringer Ingelheim International GmbH (BI).

Data availability statement The datasets used and/or analysed during the current study are available from the corresponding author on reasonable request.

Declarations

Conflict of interest SK, GS, GS, VV and MAG are employees of Boehringer Ingelheim.

Ethics All animals were housed in isolated ventilated cages under a 12-h light–dark cycle and received food and water *ad libitum*. All animal experimentation was conducted in accordance with German national guidelines and legal regulations.

Consent for publication Not applicable.

Open Access This article is licensed under a Creative Commons Attribution 4.0 International License, which permits use, sharing, adaptation, distribution and reproduction in any medium or format, as long as you give appropriate credit to the original author(s) and the source, provide a link to the Creative Commons licence, and indicate if changes were made. The images or other third party material in this article are included in the article's Creative Commons licence, unless indicated otherwise in a credit line to the material. If material is not included in the article's Creative Commons licence and your intended use is not permitted by statutory regulation or exceeds the permitted use, you will need to obtain permission directly from the copyright holder. To view a copy of this licence, visit <http://creativecommons.org/licenses/by/4.0/>.

References

1. Flume PA, Chalmers JD, Olivier KN. Advances in bronchiectasis: endotyping, genetics, microbiome, and disease heterogeneity. *Lancet*. 2018;392:880–90.
2. Ringshausen FC, Rademacher J, Pink I, de Roux A, Hickstein L, Ploner T, Welte T, Diel R. Increasing bronchiectasis prevalence in Germany, 2009–2017: a population-based cohort study. *Eur Respir J*. 2019;54:1900499.
3. Kwak HJ, Moon JY, Choi YW, Kim TH, Sohn JW, Yoon HJ, Shin DH, Park SS, Kim SH. High prevalence of bronchiectasis in adults: analysis of CT findings in a health screening program. *Tohoku J Exp Med*. 2010;222:237–42.
4. Imam JS, Duarte AG. Non-CF bronchiectasis: orphan disease no longer. *Respir Med*. 2020;166: 105940.
5. Chotirmall SH, Chalmers JD. Bronchiectasis: an emerging global epidemic. *BMC Pulm Med*. 2018;18:76.
6. Boucher RC. Muco-obstructive lung diseases. *N Engl J Med*. 2019;380:1941–53.
7. Zheng L, Shum H, Tipoe GL, Leung R, Lam WK, Ooi GC, Tsang KW. Macrophages, neutrophils and tumour necrosis factor- α expression in bronchiectatic airways *in vivo*. *Respir Med*. 2001;95:792–8.
8. Dente FL, Bilotta M, Bartoli ML, Bacci E, Cianchetti S, Latorre M, Malagrino L, Nieri D, Roggi MA, Vagaggini B, Paggiaro P. Neutrophilic bronchial inflammation correlates with clinical and functional findings in patients with noncystic fibrosis bronchiectasis. *Mediat Inflamm*. 2015;2015: 642503.
9. Craig A, Mai J, Cai S, Jeyaseelan S. Neutrophil recruitment to the lungs during bacterial pneumonia. *Infect Immun*. 2009;77:568–75.
10. Oriano M, Amati F, Gramegna A, De Soyza A, Mantero M, Sibilla O, Chotirmall SH, Voza A, Marchisio P, Blasi F, Aliberti S. Protease-antiprotease imbalance in bronchiectasis. *Int J Mol Sci*. 2021;22:5996.
11. Polverino E, Rosales-Mayor E, Dale GE, Dembowski K, Torres A. The role of neutrophil elastase inhibitors in lung diseases. *Chest*. 2017;152:249–62.
12. Witko-Sarsat V, Halbwachs-Mecarelli L, Schuster A, Nusbaum P, Ueki I, Canteloup S, Lenoir G, Descamps-Latscha B, Nadel JA. Proteinase 3, a potent secretagogue in airways, is present in cystic fibrosis sputum. *Am J Respir Cell Mol Biol*. 1999;20:729–36.
13. Sinden NJ, Stockley RA. Proteinase 3 activity in sputum from subjects with α -1-antitrypsin deficiency and COPD. *Eur Respir J*. 2013;41:1042–50.
14. Guyot N, Wartelle J, Malleret L, Todorov AA, Devouassoux G, Pacheco Y, Jenne DE, Belaouaj A. Unopposed cathepsin G, neutrophil elastase, and proteinase 3 cause severe lung damage and emphysema. *Am J Pathol*. 2014;184:2197–210.

15. Chalmers JD, Hill AT. Mechanisms of immune dysfunction and bacterial persistence in non-cystic fibrosis bronchiectasis. *Mol Immunol*. 2013;55:27–34.
16. Chalmers JD, Smith MP, McHugh BJ, Doherty C, Govan JR, Hill AT. Short- and long-term antibiotic treatment reduces airway and systemic inflammation in non-cystic fibrosis bronchiectasis. *Am J Respir Crit Care Med*. 2012;186:657–65.
17. Amitani R, Wilson R, Rutman A, Read R, Ward C, Burnett D, Stockley RA, Cole PJ. Effects of human neutrophil elastase and *Pseudomonas aeruginosa* proteinases on human respiratory epithelium. *Am J Respir Cell Mol Biol*. 1991;4:26–32.
18. Fischer BM, Voynow JA. Neutrophil elastase induces MUC5AC gene expression in airway epithelium via a pathway involving reactive oxygen species. *Am J Respir Cell Mol Biol*. 2002;26:447–52.
19. Tsang KW, Chan K, Ho P, Zheng L, Ooi GC, Ho JC, Lam W. Sputum elastase in steady-state bronchiectasis. *Chest*. 2000;117:420–6.
20. Abo-Leyah H, Gao Y, Richardson H, Keir H, Dicker A, Moffitt K, Shoemark A, Chalmers J. Proteinase-3 as a biomarker of exacerbations in bronchiectasis. *Eur Respir J*. 2020;56:3328.
21. Fazleen A, Wilkinson T. The emerging role of proteases in alpha(1)-antitrypsin deficiency and beyond. *ERJ Open Res*. 2021;7:00494–2021.
22. Adkison AM, Raptis SZ, Kelley DG, Pham CT. Dipeptidyl peptidase I activates neutrophil-derived serine proteases and regulates the development of acute experimental arthritis. *J Clin Invest*. 2002;109:363–71.
23. Vago JP, Tavares LP, Sugimoto MA, Lima GL, Galvao I, de Caux TR, Lima KM, Ribeiro AL, Carneiro FS, Nunes FF, et al. Pro-resolving actions of synthetic and natural protease inhibitors are mediated by annexin A1. *J Immunol*. 2016;196:1922–32.
24. Kohri K, Ueki IF, Nadel JA. Neutrophil elastase induces mucin production by ligand-dependent epidermal growth factor receptor activation. *Am J Physiol Lung Cell Mol Physiol*. 2002;283:L531–540.
25. Park J-A, He F, Martin LD, Li Y, Chorley BN, Adler KB. Human neutrophil elastase induces hypersecretion of mucin from well-differentiated human bronchial epithelial cells in vitro via a protein kinase C δ -mediated mechanism. *Am J Pathol*. 2005;167:651–61.
26. Polverino E, Goeminne PC, McDonnell MJ, Aliberti S, Marshall SE, Loebinger MR, Murriss M, Canton R, Torres A, Dimakou K, et al. European Respiratory Society guidelines for the management of adult bronchiectasis. *Eur Respir J*. 2017;50 (3):1700629
27. Hill AT, Sullivan AL, Chalmers JD, De Soyza A, Elborn JS, Floto RA, Grillo L, Gruffydd-Jones K, Harvey A, Haworth CS, et al. British Thoracic Society guideline for bronchiectasis in adults. *BMJ Open Respir Res*. 2018;5: e000348.
28. Keir HR, Shoemark A, Dicker AJ, Perea L, Pollock J, Giam YH, Suarez-Cuartin G, Crichton ML, Lonergan M, Oriano M, et al. Neutrophil extracellular traps, disease severity, and antibiotic response in bronchiectasis: an international, observational, multicohort study. *Lancet Respir Med*. 2021;9:873–84.
29. A study to assess the efficacy, safety, and tolerability of brensocatib in participants with non-cystic fibrosis bronchiectasis (ASPEN). NCT04594369. <https://www.clinicaltrials.gov/study/NCT04594369?term=NCT04594369&rank=1>. Accessed 03 Aug 2023.
30. Palmer R, Maenpaa J, Jauhainen A, Larsson B, Mo J, Russell M, Root J, Prothon S, Chialda L, Forte P, et al. Dipeptidyl peptidase 1 inhibitor AZD7986 induces a sustained, exposure-dependent reduction in neutrophil elastase activity in healthy subjects. *Clin Pharmacol Ther*. 2018;104:1155–64.
31. Chalmers JD, Haworth CS, Metersky ML, Loebinger MR, Blasi F, Sibila O, O'Donnell AE, Sullivan EJ, Mange KC, Fernandez C, et al. Phase 2 trial of the DPP-1 inhibitor brensocatib in bronchiectasis. *N Engl J Med*. 2020;383:2127–37.
32. Doyle K, Lonn H, Kack H, Van de Poel A, Swallow S, Gardiner P, Connolly S, Root J, Wikell C, Dahl G, et al. Discovery of second generation reversible covalent DPP1 inhibitors leading to an oxazepane amidoacetonitrile based clinical candidate (AZD7986). *J Med Chem*. 2016;59:9457–72.
33. Nuckolls GH, Slavkin HC. Paths of glorious proteases. *Nat Genet*. 1999;23:378–80.
34. Miller BE, Mayer RJ, Goyal N, Bal J, Dallow N, Boyce M, Carpenter D, Churchill A, Heslop T, Lazaar AL. Epithelial desquamation observed in a phase I study of an oral cathepsin C inhibitor (GSK2793660). *Br J Clin Pharmacol*. 2017;83:2813–20.

Publisher's Note Springer Nature remains neutral with regard to jurisdictional claims in published maps and institutional affiliations.